

Bulk crystallisation of indomethacin from simple and complex solvents

Paul A. Slavin^{a,c}, David B. Sheen^{a,d}, Evelyn E. A Shepherd^{a,*}, John N. Sherwood^{a,*}, Ranko M. Vrcelj^{a*}

Neil Feeder^{b,d}, Snezana Milojevic^{b,e}

a Department of Pure and Applied Chemistry, University of Strathclyde, Glasgow G1 1XL, Scotland, UK

b Pfizer Central Research, Sandwich CT13 9NJ, England, UK

*Corresponding author. E-mail: rankovrcelj@gmail.com

(R.M. Vrcelj)

♦ E.E.A.S. Deceased on February 25, 2018

★ J.N.S. Deceased on December 4, 2020

Current addresses:

c: GSK, London, WC1A 1DG, UK

d: Retired

e: 4056 Basel, Switzerland

Abstract

Bulk crystallisation is the commonest method for the high-volume production of pharmaceutical ingredients. As the complexity of both active pharmaceutical ingredient and solvents increases, the behaviour of the solute within the solvents may also increase in complexity. This paper compares the nucleation and growth processes of a pharmaceutical ingredient, indomethacin in three solvents, which span the range of simple to complex.

Much of the behaviour of indomethacin is mimicked across the solvents, with the γ form of indomethacin crystallising at low to medium supersaturations. At higher supersaturations, the complex solvents behave as do many other simple solvents in that the solvated β form of indomethacin is found.

The great differences in induction time for nucleation and growth timescales for the simple and complex solvents is considered as a function of supersaturation and viscosity and shows that transport processes within the solution play an important role in the crystallisation behaviour of indomethacin.

Introduction

Downstream processing of organic solids is a routine procedure in modern chemical industries and in particular, the crystallisation of pharmaceutical ingredients is vital to their final formulation and use. Crystallisation control allows formulators to deliver a wide range of particulates, with a range of properties, for example, crystalline phase and particle size. However, it is also common knowledge that crystallisation is not a totally reproducible process and that even under as stringent a set of control parameters as possible, differing particle size ranges and even crystalline phases can be produced during industrial processes. An understanding and control of crystallisation processes is critical to the successful product design in the pharmaceutical sector.

A well-established ingredient is the anti-pyretic and anti-inflammatory drug indomethacin ($C_{19}H_{16}ClNO_4$), which is used in many pharmaceutical preparations to treat patients suffering from arthritis, bursitis and tendinitis [1,2] Despite its utility and the need to understand the crystallisation processes, little has been published in this field. As the number and complexity of modern pharmaceutical ingredients increases, the range of solvents required for processing also widens from water and simple organic solvents to more complex solvents and oils which are now routinely used in downstream processing.

The exploration of nucleation and crystallisation in more complex solvents and solvent combinations can be critical in the design of dosage forms beyond standard immediate release tablets as well as informing product design in the veterinary medicines and agrochemical sectors.

Indomethacin (INC, Figure 1) exhibits complex structural behaviours. Only two polymorphs, usually referred to as Forms I (γ phase, CCDC references INDMET, INDMET01, INDMET03) [3] and II (α phase, CCDC references INDMET02, INDMET04), [4] are regularly obtainable and have had their structures characterised. The remainder exist only in thin films grown from the melt and in the presence of co-solutes or in an amorphous state. [5-8] One of these, Form III, is almost certainly a decomposition product of the melt growth process. [9] The remainder (Forms IV, VI and VII) are metastable and transform to Forms I or II on standing or heating.

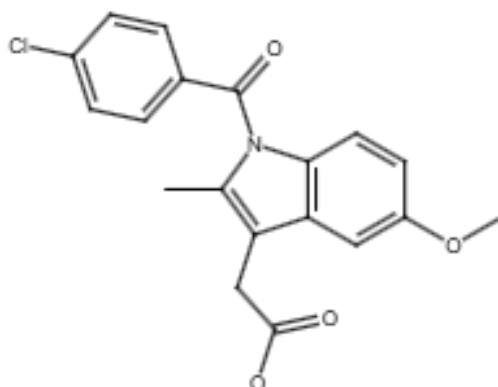


Figure 1: Molecular structure of INC

INC also shows unusual solvation behaviour. Two distinct solvated structures are known, the methanol solvate [9] (CCDC reference BANMUZ) and tert-butanol solvate [10] (CCDC references BANMOT, BANMOT01) have had their structures determined. A further set of solvated structure exists, collectively named Form V (or β phase). [5-7, 11-14] These solvates form readily from a wide range of solvents under a range of supersaturation conditions. Desolvation can lead to Forms I or II, but this can also lead to simple loss of solvent and the material retain the overall structure of Form V, effectively a “channel” solvate. Analytical methods show that the general structure of Form V is able to contain different solvents, retaining the same general crystalline structure, undergoing dilation or shrinkage depending upon the solvent. This is summarised in the electronic supplementary information (ESI) Table S1. In this study, the Greek letter nomenclature for the INC structures will be followed.

Previous studies have examined the crystallisation and morphological changes of INC that occur using a range of simple solvents, both in classic crystallisation [15] and using solvent/antisolvent processes. [16]. However, for more complex solvents little is known, hence this comparative study. Acetonitrile (C_2H_3N) is a commonly used organic solvent of low viscosity (~ 0.4 mPa.s), Ethyl oleate ($C_{20}H_{38}O_2$) is a fatty acid ester which is more viscous than acetonitrile (~ 5 mPa.s) and Miglyol 840 ($C_{39}H_{88}O_{10}$), which is an oil composed of a mixture of capric acid, octanoic acid and propylene glycol and is even more viscous (~ 10 mPa.s). Ethyl oleate and Miglyol 840 are relatively commonly used complex solvents in the pharmaceutical sector (Figure 2).

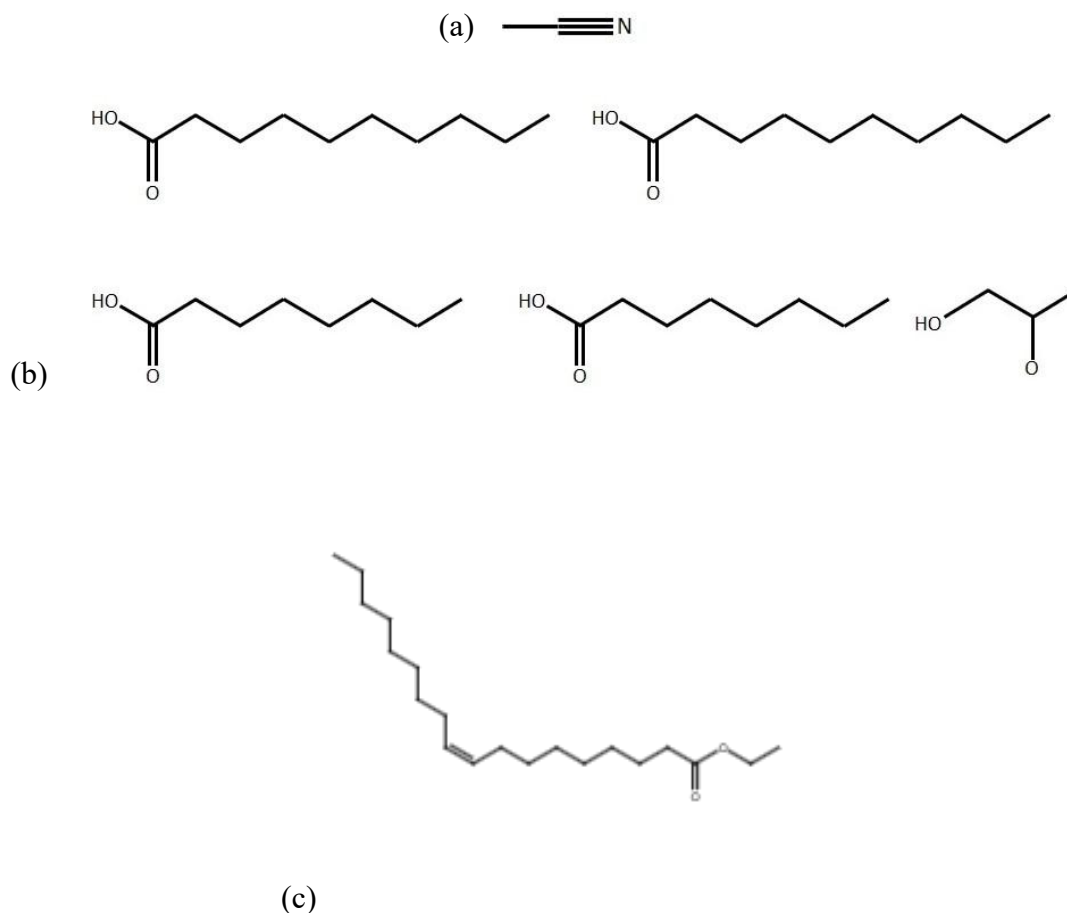


Figure 2: Molecular structures of (a) acetonitrile; (b) Miglyol 840; (c) ethyl oleate

To understand the processes occurring during crystallisation, one of the simplest and most effective ways of gaining an insight into the behaviour of solutions is to employ nucleation studies. The data obtained from these types of experiments can be manipulated to determine a number of fundamental parameters about the characteristics of a particular solution, such as interfacial tension and the critical radius (for nucleation) size. [17-20]

This study examines the crystallisation behaviour of INC in these three solvents and compares the behaviour of INC across these differing environments.

Experimental

Materials: Indomethacin [1-(p-chlorobenzoyl)-5-methoxy-2-methylindolylacetic acid], (INC), was supplied by Sigma-Aldrich Chemicals Ltd., (>99% purity) received as the γ polymorph. Acetonitrile was also obtained from Sigma-Aldrich Chemicals Ltd., (purity >99%). Miglyol

840 was supplied by Sasol Chemicals Ltd. (purity >99%) and Ethyl Oleate by Croda Chemicals Ltd. (> 99% purity). All solvents were dried over a molecular sieve and filtered through a 0.5 μm porosity PTFE membrane filter. Nujol was supplied by Sigma-Aldrich Chemicals Ltd. (M3516, Standard for Nujol mulls in IR spectroscopy).

INC was further purified by recrystallisation from HPLC grade acetonitrile (Sigma-Aldrich Chemicals Ltd., > 99.9% purity), from which γ form crystals were obtained. The crystals were filtered, dried and the purity was confirmed by microanalysis.

Solubility: Solubility measurements were carried out using the gravimetric method, with a temperature controlled saturated solution, aliquots of the solution was removed with a warmed volumetric filtered pipette, transferred to a pre-weighed sample vial, the solvent evaporated under vacuum before heating to constant weight at 70 °C. Three samples were taken at each temperature to give a final average mass value.

Nucleation studies: Nucleation was performed in an insulated 40 cm^3 glass cell with a thermostatted water jacket and isolated from ambient light sources. The cell temperature was controlled using a Haake C35 circulating bath. The internal temperature of the cell was measured by a Pt100 platinum resistance probe thermometer connected via a Picotech™ ADC16 signal conditioner and recorded digitally.

Nucleation was monitored by recording the transparency of the solution with a colorimeter (Brinkman PC700) and stainless-steel fibre optic probe. The probe was inserted into the nucleation cell and data recorded digitally. The solution in the cell was stirred at 250 rpm until precipitation had occurred. Full details of the nucleation experiments are given in ESI.

Powder X-ray Diffraction (PXRD): PXRD was performed on a Siemens D500 diffractometer in Bragg-Brentano geometry, with $\text{Cu-K}\alpha$ radiation and a graphite post-sample monochromator. Scans were taken over a range of 2θ values from 3° to 37° using a step scan mode.

Scanning Electron Microscopy (SEM): A JOEL JSM-35 Scanning Electron Microscope with an accelerating voltage of 20 kV and a probe current of 3×10^{-10} A was used and the samples coated with gold prior to examination.

Fourier Transform Infra-Red Spectroscopy (FTIR): FTIR was carried out on the Mattson 5000 FTIR spectrometer. 64 scans were collected for each sample at a resolution of 2cm^{-1} over the

wavenumber region from 4000 to 400 cm^{-1} . Samples were prepared using the nujol mull technique on NaCl plates.

Results

Solubility

The solubility of indomethacin between 20 and 60 °C in the three solvents is given in Figure 3. Each solubility curve monotonically increases with no obvious discontinuities typically associated with a phase transformation and diffraction studies of the residual solute in the flask confirmed that this solid phase is always γ -INC, giving confidence that no phase transformation occurred in this temperature range.

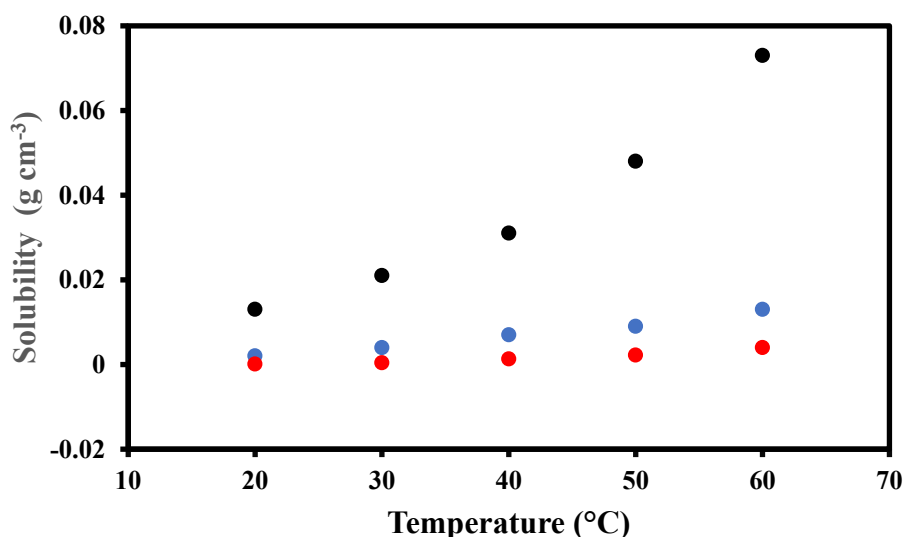


Figure 3: INC solubility in acetonitrile (black), Miglyol 840 (blue) and ethyl oleate (red)

At 30 °C the solubility of INC was approximately 23, 6 and 2 g l^{-1} in acetonitrile, Miglyol 840 and ethyl oleate, respectively. These are consistent with the solubility of INC in other organic solvents (See ESI Table S2). In the study of mixtures of alcohols and esters the solubility data was generated with the phases in the solid state being γ with an associated solid phase that was identified as β .

Polymorphism and crystal morphology

Acetonitrile: Previous work [21] has shown that in acetonitrile, INC favours the γ form at all but very high supersaturations and this was reproduced throughout these experiments where harvested material was found to be the γ form in all cases. Scanning electron micrographs (Figure 4) of the product crystals clearly shows the crystals change from block/columnar crystals at lower supersaturation to plate-like with increased supersaturation.

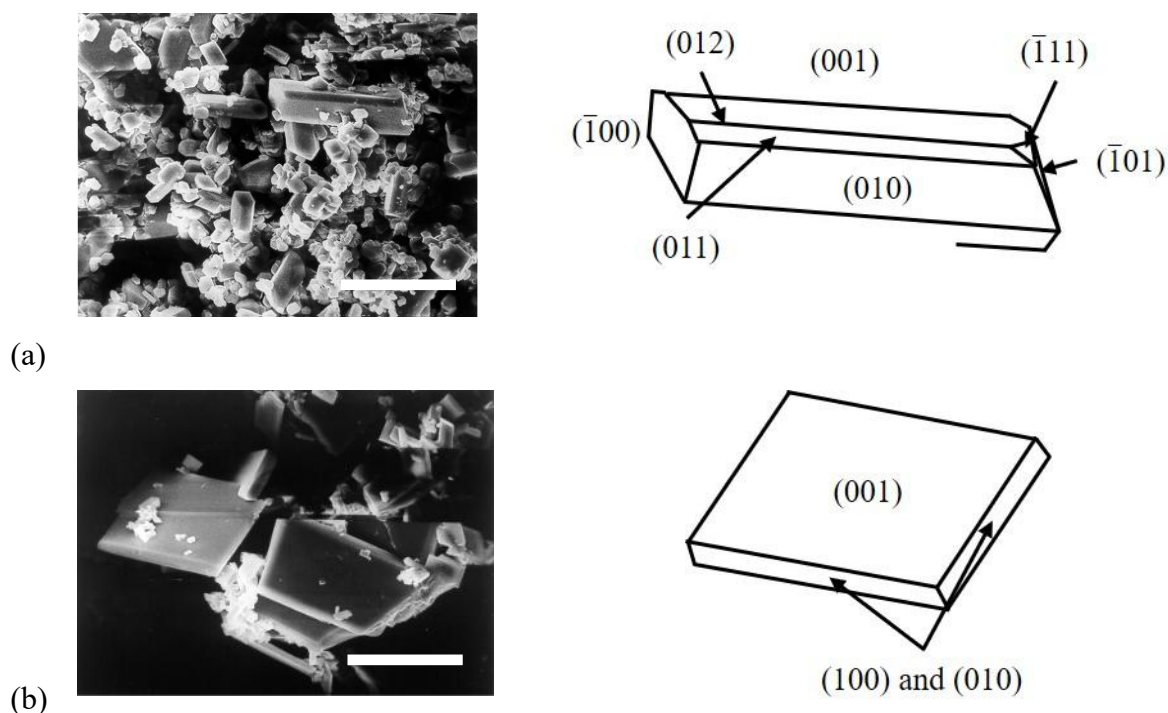


Figure 4: Scanning electron micrographs showing the change in habit of the INC crystals from columnar to plate-like with increasing supersaturation. (a) $S = 1.1$ (b) $S = 1.55$. Scale bar = 500 μm .

This variation on morphology is in agreement with that found with large crystals ($\sim 1\text{-}2\text{ cm}$). [22] At lower supersaturation the crystals are columnar, the major forms being $\{001\}$, $\{010\}$ and $\{100\}$ with smaller $\{\bar{1}01\}$ faces and the capping faces are $(\bar{1}11)$, (011) , (012) and $(\bar{1}01)$ (Figure 2a). At higher supersaturations the crystals have a plate-like appearance with the dominant $\{001\}$ faces bounded by smaller $\{100\}$ and $\{010\}$ faces.

The size distribution of the crystals varies over a wide range. The largest size crystals observed in the SEM images were up to around 1000 μm in the largest dimension. Typically, crystals were in the order of 200-300 μm in the two largest dimensions.

Miglyol 840: At low to medium supersaturations, the γ form was always recovered and the habit was identical to those produced from acetonitrile under the higher supersaturation conditions, Figure 5, with flat plates and the $\{001\}$ face dominant. Block-like shaped crystals were never observed. As INC does not nucleate in Miglyol 840 at $S < 1.3$ (within 7 working days), it is not possible to directly compare morphologies of crystals to those of Acetonitrile at similar supersaturation values. At higher supersaturations ($S > 2.5$), the β solvated form was found.

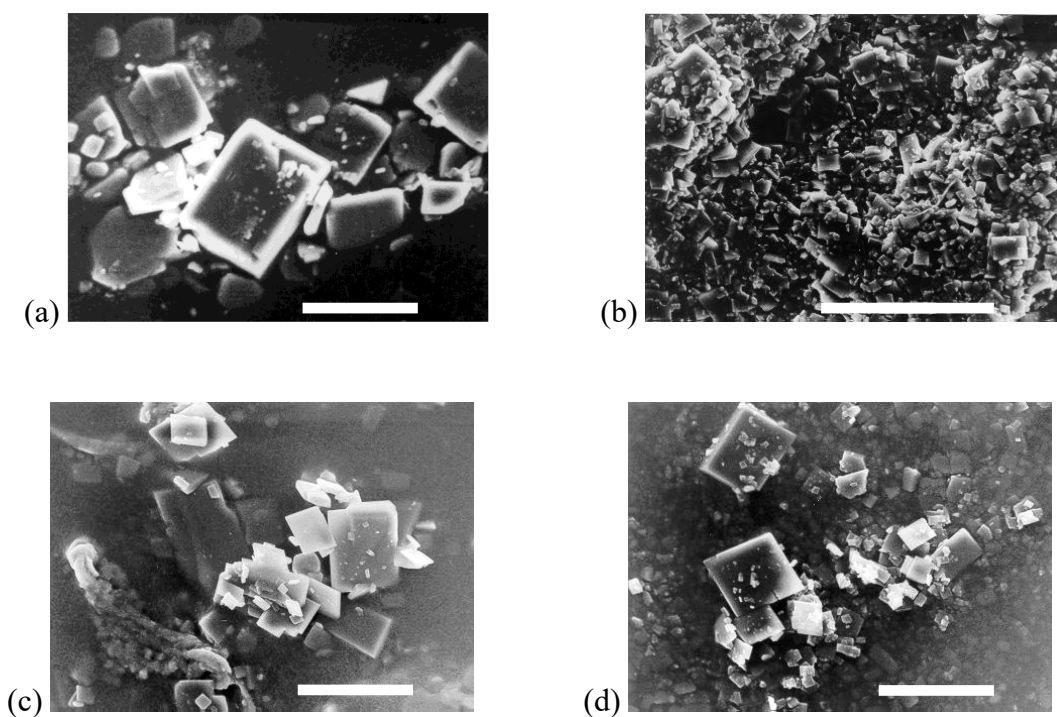


Figure 5: Scanning electron micrographs of INC crystals precipitated from Miglyol 840 (a) $S = 1.35$; (b) $S = 1.7$; (c) $S = 2.0$; (d) $S = 2.4$. Scale bar = 500 μm .

The general size of the γ form crystals is smaller than for those found from acetonitrile, with the largest size observed of ~ 500 μm in the largest two dimensions, but typically the crystals were < 100 μm in the longest dimension. Three interrelated factors could account for this, the supersaturation leads to nucleation of a larger number of crystals, combined with the crystals

not growing as well as in the case of those in acetonitrile and that the solubility is insufficient to provide sufficient material for significant growth after nucleation.

At the highest supersaturations ($S > 2.5$), equivalent to 30 K undercooling, the β solvate form is produced. Figure 6 shows a typical micrograph of this phase, compared to a known sample of the β form obtained from 2-butanol and Figure 7 shows a PXRD pattern of the material compared with an established dichloromethane solvate. It is believed that the β form has a channel-like structure and is capable of incorporating solvent, with the lattice dilating or shrinking depending upon the solvent molecule being incorporated. The presence of solvent in the crystal structure was confirmed by the FTIR data. Figure 7 compares the FTIR pattern of the solvate material obtained from Miglyol 840, the known dichloromethane solvate and pure Miglyol 840. The patterns match, with peaks at 1677 and 1697 cm^{-1} characteristic of the solvate and that at 1745 cm^{-1} characteristic of Miglyol 840.

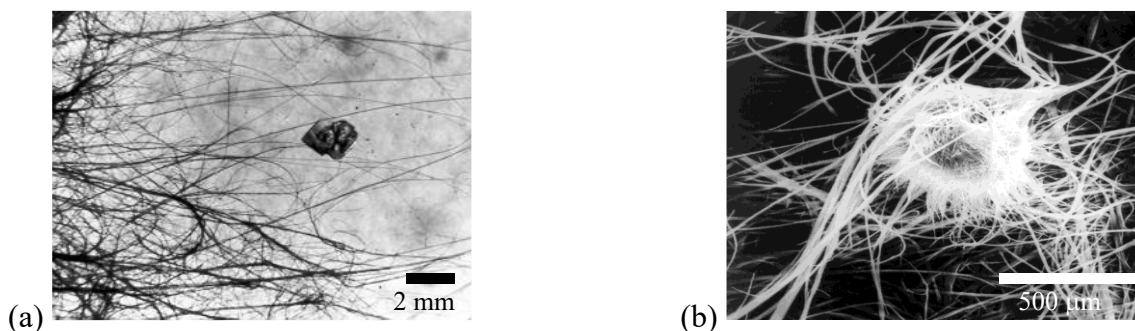


Figure 6: Optical micrograph of the solvate form precipitated from (a) 2-butanol; (b) Miglyol 840.

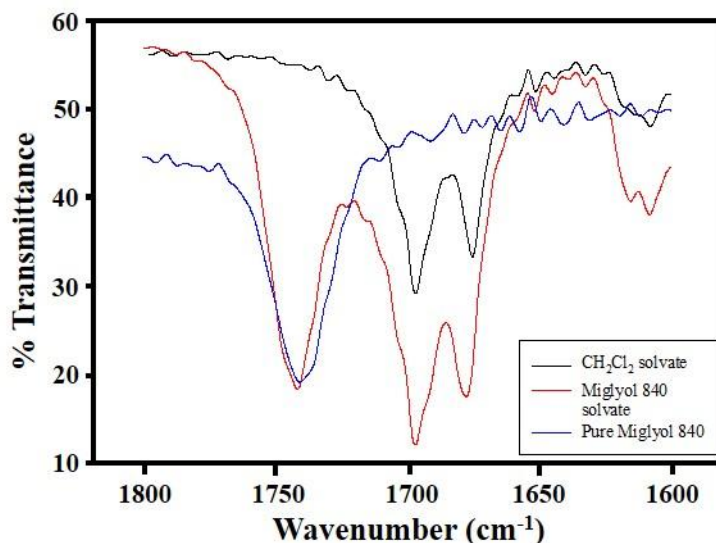


Figure 7: FTIR patterns of Miglyol 840, CH_2Cl_2 solvates and pure Miglyol 840

Ethyl oleate: For ethyl oleate, the polymorphic forms of the materials generated from the crystallisation experiments and the order of their appearance followed the pattern of Miglyol 840, with the γ form being found at low to medium supersaturations and the β solvate form found at high supersaturations ($S > 2.7$). At these higher supersaturations the solvate always precipitated. The structure and properties of the β solvate form was again found to be very similar to that the Miglyol 840 solvate and the solvates generated from all of the simple solvents. As with Miglyol 840, no nucleation occurred at the lowest values of supersaturation, so direct comparisons of the behaviour with that of acetonitrile cannot be made.

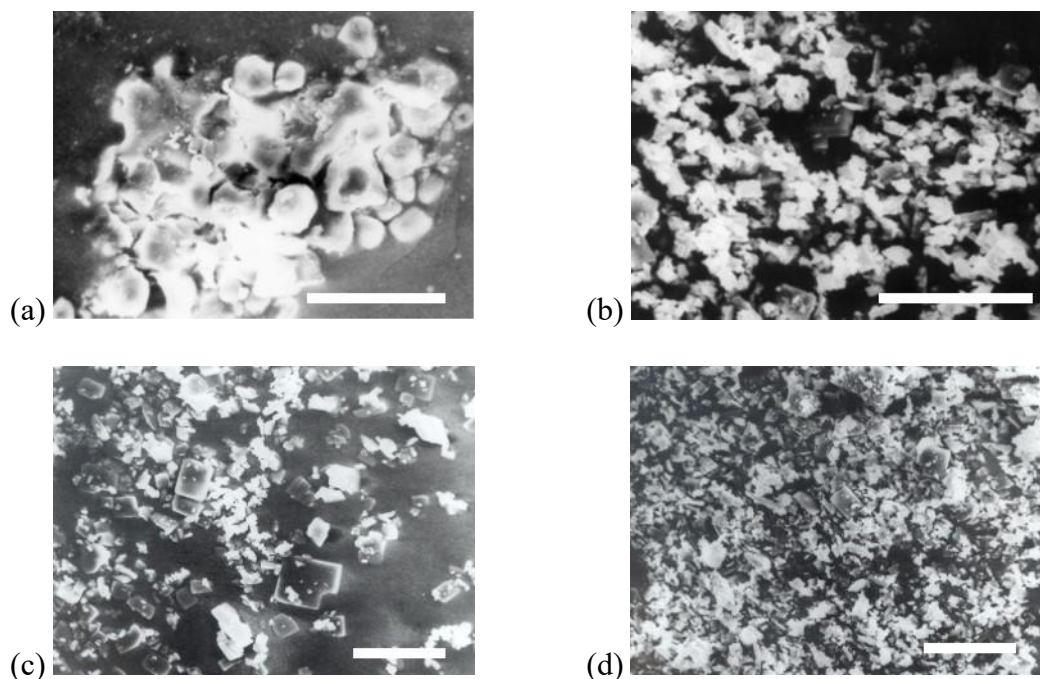


Figure 8: Scanning electron micrographs of INC crystals precipitated from ethyl oleate (a) $S = 1.4$; (b) $S = 1.65$; (c) $S = 2.15$; (d) $S = 2.55$. Scale bar = 500 μm

The γ form product crystals from the experiments in this case show some slight differences to previous recrystallisations. In general, the crystals are typical of the γ form crystals seen under most circumstances i.e., $\{001\}$ plates. The size distribution of the crystals are also similar to that of the crystals precipitated from Miglyol 840 i.e., generally less than 100 μm . The main difference is that crystals at the early precipitation stages have a rough appearance, as if they are not fully developed, this is in contrast to the normal plate-like crystals observed at the point where the solution is almost fully turbid. It would certainly appear to be the case that the number of crystals in the latter sample is greater. This is probably due to the fact that crystals at the early stages of turbidity are too small to be filtered i.e., less than 0.5 μm . The crystals grown at lower supersaturation (1.4), shown in Figure 8 look very poor quality, and the number is low. They are also similar in appearance to the crystals grown at 1.35 supersaturation from Miglyol 840 (Figure 5a). These poor crystals are reminiscent of large single crystal growth from the oils [21], where the growth rate was very low and the crystals were characterised by poor surfaces and solvent inclusion.

At higher supersaturations, crystallisations of INC from ethyl oleate behaved in a similar manner to those observed from Miglyol 840. Confirmation that the material was a β solvate

was again obtained from PXRD and FTIR patterns, Figures 9 and 10, in which a peak corresponding to the solvent itself was present.

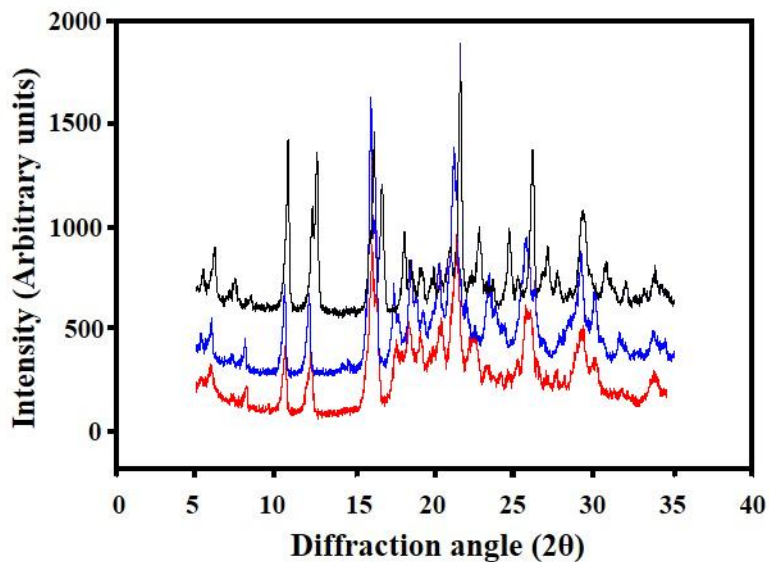


Figure 9: PXRD patterns of ethyl oleate (red), Miglyol 840 (blue) and CH₂Cl₂ (black) solvates.

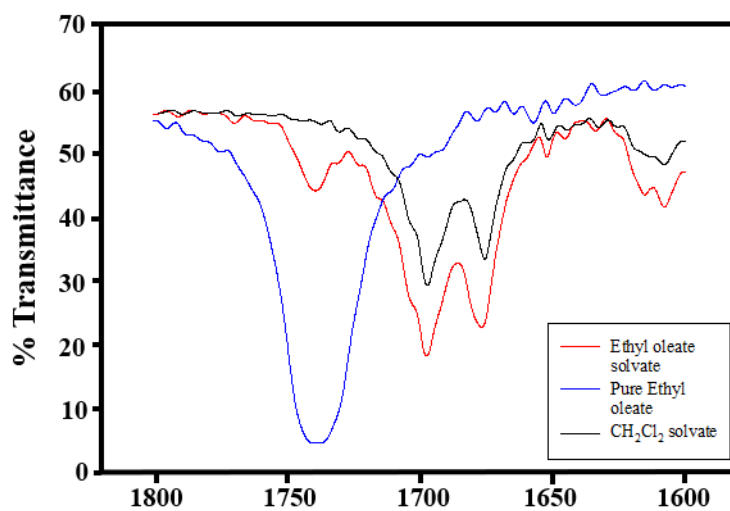


Figure 10: FTIR patterns of ethyl oleate, CH₂Cl₂ solvates and pure ethyl oleate.

Nucleation studies

The variations in induction time, τ , with supersaturation, S , for the solutions of INC in acetonitrile, Miglyol 840 and ethyl oleate, collected from 35 °C to higher temperatures are given in Figures 11a-c. The data are consistent with that of other pharmaceutical materials, e.g. paracetamol [23,24] in terms of the trends observed.

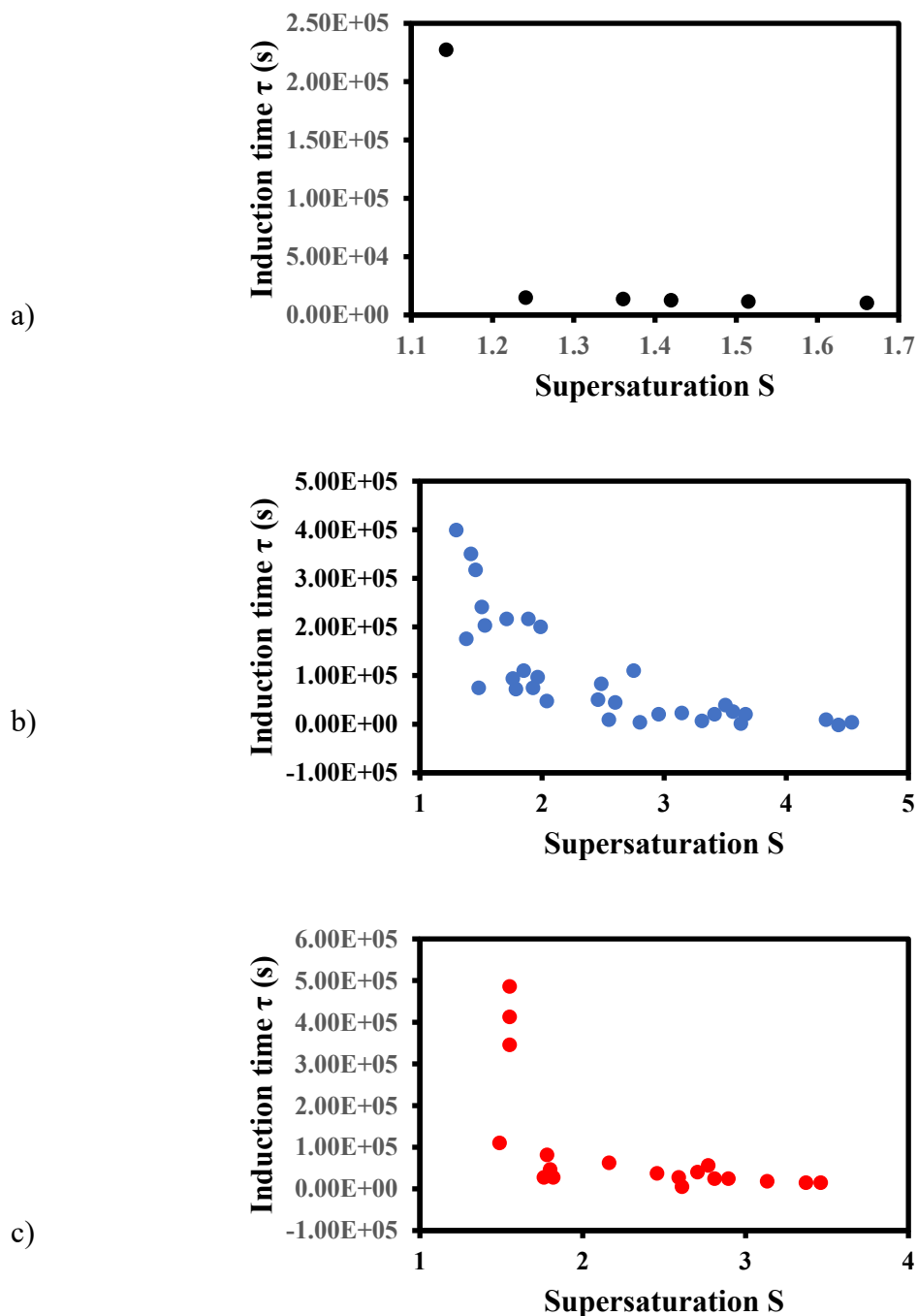


Figure 11: Variation of induction time with supersaturation for pure INC in; a) acetonitrile; b) Miglyol 840; c) ethyl oleate.

Each of the figures show that the induction time decreases markedly with increasing supersaturation, with acetonitrile showing the sharpest drop, followed by the behaviour of ethyl oleate and with Miglyol 840 showing the least steep change in induction time.

In acetonitrile, the nucleation induction time decreases markedly from ~4000 minutes at relatively low supersaturation (~1.1-1.25) to medium/higher supersaturations (1.3-1.85) and ~25 minutes at the highest end. With ethyl oleate, the induction times are much longer, although the sharpness of the transition from long to short induction times mimics the behaviour of acetonitrile. Nucleation was observed only at medium/higher supersaturations ($S > \sim 1.5$), so it is not possible to directly compare this behaviour with that, but at the lowest supersaturations where nucleation was observed the time to nucleation was ~ 6000 – 7000 minutes and ~ 300 minutes at the highest supersaturations. In Miglyol 840, this behaviour is further accentuated. Although the data is more scattered than for either acetonitrile or ethyl oleate, this is to be expected in nucleation studies. As with ethyl oleate, nucleation occurred at higher supersaturations than seen for acetonitrile, ($S > \sim 1.3$) and similarly, the time to nucleate was ~ 6000 – 7000 minutes and ~ 300 minutes at the highest supersaturations. For both Miglyol 840 and ethyl oleate, low supersaturations led to no observable nucleation after 1 week and therefore were not considered in the current study.

Discussion

Polymorphism

The polymorphic and nucleation behaviour of INC in the three solvents is dependent upon the interaction of the solute molecule with the solvent molecules. The three solvents used have different molecular structures (Figure 2), however, the polymorphic behaviour of INC in each of these is no different to the observations of INC crystallised from a range of simple solvents. In general, at low to medium supersaturations, the γ form is found, with the general morphology being consistent and at high supersaturations, the β solvated form is found.

Miglyol 840 is a mix of decanoic acid, octanoic acid and propylene glycol (in a 2:2:1 ratio), ethyl oleate is a long chain material, with an ester group and an unsaturated element, neither of which are unusual in solvent terms. Previous studies have utilized esters (ethyl acetate) and unsaturated elements (benzene, toluene), thus the chemical nature of the oils is unlikely to have

a major effect upon the crystallization behaviour of INC. Any differences in behaviour will be due to either the size or other physical characteristics of the oils.

Nucleation

According to the classical nucleation theory of Gibbs, Volmer and Becker and Döring, [25-27] the nucleation rate J is inversely proportional to the induction time τ , thus the plot of $\ln(\tau)$ vs $1/T^3(\ln S)^2$ ought to deliver a straight line with gradient:

$$m = \frac{\beta\gamma^3\Omega^2}{k^3}$$

Where β is a shape factor ($16\pi/3$ assuming a spherical nucleus), γ the surface free energy (or interfacial tension), Ω the molecular volume ($4.48 \times 10^{-28} \text{ m}^3$), and k the Boltzmann constant ($1.38 \times 10^{-23} \text{ m}^2\text{kgs}^{-2}\text{K}^{-1}$). This allows γ to be calculated and from this, an estimation of the critical radius r_{crit} can be made via:

$$r_{\text{crit}} = \frac{2\gamma\Omega}{kT \ln(S)}$$

Where $S = C/C^*$ (C and C^* are the concentrations of the supersaturated and saturated solutions, respectively).

The plots of $\ln(\tau)$ as a function of $T^{-3}(\ln S)^{-2}$ for INC in each solvent can be constructed (Figures S1a-c). Each graph shows two distinct regions. These regions are clear for the Miglyol 840 and ethyl oleate data, less so for the acetonitrile data. Although all six acetonitrile data points can be associated with a single fitted line, observations during the ongoing experiments (as noted in the description of the runs in the ESI) lead us to believe that there are differences in the behaviour of the first three runs compared to that of the last three runs. This is particularly in the distribution of the final particulates, the final three datapoints (the low supersaturation runs) have particulate distributions clearly associated with the apparatus (cell walls, stirring bar, etc.) that indicate that this is dominated by heterogeneous nucleation and growth.

At higher supersaturations (low values of $T^{-3}(\ln S)^{-2}$) the gradients are steep and are associated with homogeneous nucleation. At lower supersaturations (higher values of $T^{-3}(\ln S)^{-2}$), the gradients are distinctly less steep and are associated with heterogeneous nucleation. [28,29] As

heterogeneous nucleation is influenced by many factors, e.g. shape of vessel, stirring rates, extraneous nucleating agents, etc., the following discussion will concentrate upon homogeneous nucleation.

The calculations estimating the surface free energy and critical radius for INC in each of the three solvents are given in Table 1.

Table 1: Surface free energy values for INC in the solvents used in the study.

Solvent	$M (K^{-3}) (10^7)$	$\gamma (Jm^{-2}) (10^{-3})$
Acetonitrile	53	1.6
Ethyl Oleate	5.3	3.5
Miglyol 840	2.3	2.6

For each solvent, as the supersaturation increases, the critical radius size decreases to a level at which the supersaturation is so high that the critical nucleus size is less than 1 molecule in volume (Tables S3a-c). If one compares the critical radii sizes for similar driving forces in the simple and complex solvents it is clear that that the size of a critical nucleus in the oils is significantly larger. For example, at a driving force of around 1.3-1.35 supersaturation, the size of a critical nucleus in Miglyol 840 is approximately 75-80 molecules of INC, whereas for acetonitrile the size is around 10-15 molecules of INC. At supersaturations of $\sim 1.5 - 1.55$, for acetonitrile, the size drops to $\sim 6-8$ molecules of INC, in Miglyol 840 down to $\sim 15 - 20$ molecules of INC and in ethyl oleate, this is $\sim 45 - 55$ molecules of INC.

At the very high supersaturation levels the size of the critical nucleus in both Miglyol 840 is less than one molecule and ethyl oleate approaches that value. Whilst this could be thought of as a possible insight as to when these solutions become labile, it is much more likely to be related to a number of factors which cause this approximation to break down. In addition to the spherical nucleus estimation, at these higher supersaturation levels, heterogeneous nucleation becomes the dominant mechanism and also the polymorph that appears changes from the γ form, to the β form.

These results show the similarity of behaviour of INC whether crystallised from simple or complex solvents. The resulting morphologies and polymorph/solvate appearance is the same as that of INC crystallised from either acetonitrile or any of a wide range of simple organic solvents (17). In the particular case of acetonitrile, crystals of γ INC precipitated from low supersaturations exhibited a block like morphology, bounded by high index faces which grew out at the higher levels of supersaturation to reveal the tablet-like morphology with the dominant $\{001\}$ faces. These variations in morphology are due to the varying growth rates of the crystallographic faces and mimic the behaviour of large crystals of γ INC grown under controlled conditions, where morphology changes are due to the varying growth rates of the crystallographic faces. [22]

The fact that the solvate and γ forms precipitated and in the same order as seen previously in the simple solvents would again suggest that the effect of the molecular nature of the solvent on polymorphic form is negligible. It has been suggested that viscous solvents can favour the formation of metastable polymorphs by minimising the possibility of pre-crystallisation of more stable phases. [30] Again, we have seen no evidence of any metastable phases apart from the solvate form. There is no evidence of the α form formation. This order of crystallisation is line with what has been seen previously as the solvate being the least soluble will likely precipitate unless the kinetics of formation of the α form are favoured. In terms of the rates of formation of the two forms in the oils, the appearance of the solvate forms seems to be more rapid, as suggested by the rate of light transmittance drop. However, this can be explained in a number ways: firstly, the physical form of the solvate, (“sherbet” or “cotton wool”-like) makes it aggregate very easily, particularly around the probe. Also, it is no doubt less dense than the γ form which will add to the extra volume in the bulk. Furthermore, the higher driving forces involved in the solvate formation will lead to a greater yield of crystalline material.

This fast rate of formation is in contrast with the formation of the γ form in the oils, illustrated by comparing the growth times for the γ form crystals between the simple and complex solvents. For the same driving force the time between nucleation and 50% loss in transmittance is around 50 times longer in the oil. This is shown in Figure S2. The red data corresponds to the light transmittance profile for the nucleation and growth of INC in acetonitrile at a supersaturation of approximately 1.7. The black data corresponds to the similar profile for INC

in Miglyol 840 at the same supersaturation. Two axes have been used because the timescales are so vastly different.

Whilst INC shows many similarities in the different solvents, initial nucleation and growth and secondary nucleation processes in acetonitrile is fast, such that less than 10% light transmittance is observed after a relatively short period of time. This is not unexpected as crystal growth is a fast process in comparison to nucleation, particularly at higher supersaturations. [20] In contrast, for the oil-based solutions the same process after initial nucleation takes what may appear to be an unexpectedly long time.

The clear difference is the solubility of INC in each medium. The solubility of INC in Miglyol 840 is around 4 times less than in acetonitrile, and in ethyl oleate it is around 10 times less soluble and intuitively a delay is what would be expected; however, the delay is much greater than a simple 4- or 10-times difference in time, even with the differences in solubility.

However chemical make-up can also be important, in general terms, when the composition of a solution is changed such that the solubility decreases, this leads to an increase in the interfacial tension between the crystal and the surrounding medium. [31]

Inspection of the various parameters calculated for the three solvents, in conjunction with the above equation, illustrates why the rate of nucleation in the complex solvents is much lower than in the simple solvent (Table 2). As it can be seen there is a considerable increase in the interfacial tension between the crystal nuclei and the bulk solution as the solubility decreases. This, in turn, leads to a significant increase in the critical radius size, as r_{crit} is proportional to γ . The normalised relative nucleation rates have been estimated and are also in line with the observations. The nucleation rate in acetonitrile is more than four orders of magnitude higher than in ethyl oleate.

Apart from the “normal” factors which affect the nucleation rate, such as those discussed above, another potentially important factor which is not specifically considered in any of the theoretical treatment of nucleation theory is the viscosity of the bulk medium. This would be expected to affect molecular transport and mobility and have an effect on nucleation and crystal growth.

Table 2: Various parameters for INC in each solvent. Solvent abbreviations (A) Acetonitrile; (M) Miglyol 840; (EO) Ethyl oleate.

Solvent	Rel. Sol.	γ (mJ m ⁻²)	r_{crit} at ~50% supersatn. (Å)	Number of molecules per r_{crit}	Rel. nucln. rate at ~50% supersatn.
A	High	1.61	8.44	5.82	26117
M	Medium	2.64	12.34	18.17	825
EO	Low	3.47	16.24	41.42	1

Figure S3 shows the viscosity of the two oils utilised in this study together with that of acetonitrile. The y-axis scale on the right corresponds to the viscosity of acetonitrile [32] for clarity as the scales are very different. As it can be seen, the viscosity of acetonitrile is more than a magnitude lower than that of the two oils.

The effect of viscosity has been considered by Zettlemoyer, [33] and Turnbull and Fisher, [34] and investigated experimentally by Mullin et al. [35] on highly concentrated aqueous solutions of citric acid. They found that the nucleation rate went through a maximum as the undercooling (supersaturation) and viscosity increases. This has also been observed by Franks and co-workers in the nucleation of ice crystals. [36]

The frequency of atomic or molecular transport at the nucleus-liquid interface, v , can be related to the bulk viscosity, η , by the Stokes-Einstein equation. [37]

$$v \approx \frac{kT}{3\pi a_0^3 \eta(T)}$$

where a_0 is the mean effective diameter of the diffusing species. Therefore, the effect on v of the complex solvents is clear. Since the viscosity is inversely proportional to the molecular transport parameter, v , then as the viscosity increases the molecular transport and mobility will decrease.

After nucleation, the growth rate is then a balance between diffusional steps in which the solute is transported from the bulk fluid through the solution boundary layer adjacent to the crystal surface, and an integration (“deposition”) step in which the adsorbed solute at the crystal surface is deposited and integrated into the crystal lattice. [38-41]

In this study, it is not possible to further define the balance of the diffusional and integrational steps, nor to define which of the two factors controls, nor define D_a , the Damköhler number for crystal growth. [42]

That there is a relationship between all of these factors and the influence of the solution (in this case the more complex solvents) on the growth of the crystals after nucleation is clear given the highly extended nucleation and growth times for INC in the complex solvents, compared to its behaviour in simple solvents, characterised both in this work and earlier observations. [21]

Conclusion

From the data gathered in the nucleation studies and examined in conjunction with the outcomes of the previous experiments it would appear that the effect of a complex solvent on the crystallisation of INC from solution is related to nothing more than to the physical properties of the solvent, and the restrictions these physical properties impart on the system.

From the nucleation studies the crystalline product was identical to that observed in the simple solvents. In the case of acetonitrile, the only polymorph that precipitated was the γ form which was expected, given the supersaturation range examined. The morphology of the product crystals was similar to that observed in the growth of the large single crystals and can be explained by the supersaturation dependent growth rate of the various crystallographic faces.

From the two oils the β solvate form precipitated at very high supersaturations and the γ form at low to medium/high supersaturations, as found by Slavin et al [21], where in a number of solvents the β solvate would preferentially form at high driving forces and the γ form under all other conditions. The structure of the oil solvates would appear to be isomorphous with the other solvates grown from the simple solvents, apart from some small differences in lattice

spacings which is to be expected as the solvent molecules are very large. The exact stoichiometry of the solvates was difficult to define exactly but has been shown to be lower than the simple solvates, in line with the fact that molecule is significantly larger. Hence mole for mole there will be less per mole of INC than a smaller solvent. The γ form crystals that precipitated were identical {001} plates to those observed in all other solvents and from melt crystallisation. These observations prove that the dominant forces in solution are those of the solute-solute interactions.

From the induction time studies various parameters for homogeneous nucleation were calculated and it was found that these parameters suggested nucleation in the oils was significantly more difficult, for equivalent driving forces. These factors are strongly dependent on solubility and the solubility of INC in the oils is significantly less than in acetonitrile. Other factors such as viscosity have been considered and in a qualitative sense have been shown to be important.

After nucleation it was found that the crystal growth process in the oils was also significantly slower in the complex solvents. In Miglyol 840 it was found that for the same supersaturation the time to reach 50% loss in light transmission was around 50 times longer than in acetonitrile. This has been rationalised in terms of the various factors which affect solute transport between the bulk and the interface and not the crystal growth process itself. The close similarity between the morphology of the crystals grown from a range of solvents, simple and complex, and the melt suggest that this is independent of the medium. This behaviour of the growth of IMC from different solvent types bears a striking resemblance to the nucleation behaviour of posaconazole from the melt, which, when doped with chemically different and distinct surfactants, does not affect the surface/solute interface and only affect the nucleation rates. [43]

The different forms of IMC will affect the solubility, our value of the solubility of IMC in Miglyol 840 compares well with the work by Czajkowska-Kośnik and Sznitowska [44], their study is not focussed on nucleation and crystal growth. It is clear from the complex solvents considered in this study that the main effect on the crystallisation process of a complex solvent are the physical limitations the solvent imposes on the system, the main factor is molecular size which leads to a greater viscosity which, in turn, influences solubility, hydrodynamics and molecular diffusion.

Electronic Supplementary Information

The ESI contains additional information of INC polymorphism and solubility, nucleation data, critical radius estimates, light transmittance data, viscosity information and detailed nucleation experimental information. (ESI.doc).

Acknowledgements

We acknowledge the kind support of Pfizer Central Research UK for their financial support of this work and Robert Docherty in particular for his insightful comments on this manuscript. PAS wishes to express his gratitude for Pfizer's financial support of his PhD studies.

References

1. Shen T. Y.; Ellis R. L.; Windholz T. B.; Matzuk A. R.; Rosegay A.; Lucas S.; Witzel B. E.; Stammer C. H.; Wilson A. N.; Holly F. W.; Willet J. D.; Sarret L. H.; Holtz W. J.; Risely E. A.; Nuss G. W.; Winter C. A. Non-Steroid Anti-Inflammatory Agents. *J. Am. Chem. Soc.* **1963**, 85, 488 - 489.
2. Winter. C. A.; Risley E. A.; Nuss G. W. Anti-Inflammatory and Antipyretic Activities of Indo-methacin, 1-(*p*-chlorobenzoyl)-5-methoxy-2-methyl-indole-3-acetic acid. *J. Pharm. Exptl. Therap.* **1963**, 141, 369 – 376.
3. Kistenmacher. T. J.; Marsh R. E. Crystal and molecular structure of an antiinflammatory agent, indomethacin, 1-(*p*-chlorobenzoyl)-5-methoxy-2-methylindole-3-acetic acid. *J. Am. Chem. Soc.* **1972**, 94, 1340 – 1345.
4. Chen X.; Morris K. R. Griesser U. J.; Byrn S. R.; Stowell J. G. Reactivity Differences of Indomethacin Solid Forms with Ammonia Gas. *J. Am. Chem. Soc.* **2002**, 124, 15012 – 15019.
5. Borka L. The polymorphism of indomethacine. New modifications, their melting behavior and solubility. *Acta. Pharm. Suecica.* **1974**, 11, 295 – 303.
6. Lin S. Y. Isolation and solid-state characteristics of a new crystal form of indomethacin. *J. Pharm. Sci.* **1992**, 81, 572 – 576.
7. Lin S. Y.; Cherng J. Y. Polymorphic transformation of indomethacin in precirol solid dispersion system. *J. Therm. Anal.* **1995**, 45, 1565 – 1577.

8. Yoshioka. M.; Hancock B. C.; Zografi G. Crystallization of indomethacin from the amorphous state below and above its glass transition temperature. *J. Pharm. Sci.* **1994**, *83*, 1700 – 1705.
9. Joshi. V.; Stowell J. G.; Byrn S. R. Solid-State Stability of Indomethacin Solvates. *Mol. Cryst. Liq. Cryst.* **1998**, *313*, 265 – 270.
10. Cox P. J.; Manson P. L. Indomethacin *tert*-butanol solvate at 120 K. *Acta Crystallogr.* **2003**, *E59*, o1189 – o1191.
11. Gałdecki Z.; Glówka M. L.; Górkiewicz Z. Examination of polymorphism of 1-(*p*-chlorobenzoyl)-5-methoxy-2-methylindolyl-3-acetic acid. *Acta. Pol. Pharm.* **1977**, *34*, 521 – 525.
12. Yamamoto H. 1-Acyl-indoles. II. A New Syntheses of 1-(*p*-chlorobenzoyl)-5-methoxy-3-indolylacetic Acid and Its Polymorphism. *Chem. Pharm. Bull.* **1968**, *16*, 17 – 19.
13. Pakula R.; Pichnej L.; Sychala S.; Butkiewicz K. Polymorphism of indomethacin. Part I. Preparation of polymorphic forms of indomethacin. *Pol. J. Pharmacol. Pharm.* **1977**, *29*, 151 – 156.
14. Sychala. S.; Butkiewicz K.; Pakula R.; Pichnej L. Polymorphism of indomethacin. Part II. Identification and rapid determination of polymorphic forms of indomethacin by IR spectrometry. *Pol. J. Pharmacol. Pharm.* **1977**, *29*, 157 – 160.
15. Malwade C. R.; Qu H. Cooling Crystallization of Indomethacin: Effect of Supersaturation, Temperature, and Seeding on Polymorphism and Crystal Size Distribution. *Org. Process Res. Dev.* **2018**, *22*, 6, 697–706
16. Hugo Silva M.; Kumar A.; Hodnett B. K.; Tajber L.; Holm R.; Hudson S. P. Impact of Excipients and Seeding on the Solid-State Form Transformation of Indomethacin during Liquid Antisolvent Precipitation. *Cryst. Growth Des.* **2022**, *22*, 6056–6069
17. Meenan P.; Roberts K. J. The application of an automated crystallization cell used to study the nucleation kinetics of potash alum. *J. Mat. Sci. Lett.* **1993**, *12*, 1741 – 1744.
18. Gerson A. R.; Roberts K. J.; Sherwood J. N. An instrument for the examination of nucleation from solution and its application to the study of precipitation from diesel fuels and solutions of *n*-alkanes. *Powd. Tech.* **1991**, *65*, 243 - 249.
19. Nielsen A. E.; Söhnel O. Interfacial tensions electrolyte crystal-aqueous solution, from nucleation data. *J. Cryst. Growth.* **1971**, *11*, 233 – 242.

20. Roberts K. J.; Sherwood J. N.; Stewart A. The nucleation of n-eicosane crystals from solution in n-dodecane in the presence of homologous impurities. *J. Cryst. Growth.*, **1990**, 102, 419 – 426.
21. Slavin P. A.; Sheen D. B.; Shepherd E. E. A.; Sherwood J. N.; Feeder N.; Docherty R.; Milojevic S. Morphological evaluation of the g-polymorph of indomethacin. *J. Cryst. Growth.* **2002**, 237 – 239, 300 – 305.
22. Slavin P. A. PhD Thesis, Crystallisation and polymorphism of the pharmaceutical Indomethacin from simple and complex solvents 2003, University of Strathclyde
23. Prasad K. V. R.; Ristic R. I.; Sheen D. B.; Sherwood J. N. Crystallization of paracetamol from solution in the presence and absence of impurity. *Int. J. Pharm.*, **2001**, 215, 29 – 44.
24. Granberg R. A.; Ducreux C.; Gracin S.; Rasmuson Å. C. Primary nucleation of paracetamol in acetone–water mixtures. *Chem. Eng. Sci.*, **2001**, 56, 2305 – 2313.
25. Gibbs J. W., *Collected Works (Vol. I), Thermodynamics*, Yale University Press, 1948.
26. Volmer M., *Kinetic der Phasenbildung*, Steinkopff, Leipzig, 1939.
27. Becker R.; Döring W. Kinetische behandlung der keimbildung in übersättigten Dämpfen. *Annalen der Physik* **1935**, 24, 719 – 752.
28. Mullin J. W., *Crystallisation* (3rd Ed.), Butterworth-Heinemann, 1993.
29. Myerson A. S., *Handbook of Industrial Crystallisation* (2nd Ed.), Butterworth-Heinemann, 2002.
30. Threlfall T. Crystallisation of Polymorphs: Thermodynamic Insight into the Role of Solvent. *Org. Process. Res. Dev.* **2000**, 4, 384 – 390.
31. Nývlt J.; Söhnel O.; Matuchová M.; Broul M. *The Kinetics of Industrial Crystallisation*, Elsevier, 1985
32. Riddick J. A.; Bunger W. B.; Sakano T. K. *Organic Solvents and Physical Methods of Purification in Techniques of Chemistry*, Wiley, 1986, Volume 2.
33. Zettlemoyer A. C., *Nucleation*, Marcel Dekker, 1969.
34. Turnbull D.; Fisher J. C. Rate of Nucleation in Condensed Systems. *J. Chem. Phys.* **1949**, 17, 71 – 73.
35. Mullin J. W.; Leci C. Some nucleation characteristics of aqueous citric acid solutions. *J. Cryst. Growth.*, **1969**, 5, 75 – 76.
36. Franks F.; Mathias S. F.; Trafford K. The nucleation of ice in undercooled water and aqueous polymer solutions. *Coll. Surf.*, **1984**, 11, 275 – 285.

37. Rodríguez-Hornendo R.; Murphy D. Significance of controlling crystallization mechanisms and kinetics in pharmaceutical systems. *J. Pharm. Sci.*, **1999**, 88, 651 – 660.
38. Garside J.; Mersmann A.; Nyvlt J. *Measurement of Crystal Growth and Nucleation Rates* (2nd Ed.), Institution of Chemical Engineers, 2002.
39. Richardson J. F.; Harker J. H.; Backhurst J. R. *Coulson and Richardson's Chemical Engineering Vol. 2: Particle Technology and Separation Processes* (5th Ed.), Butterworth-Heinemann, 2002.
40. Garside J. The concept of effectiveness factors in crystal growth. *J. Chem. Eng. Sci.*, **1971**, 26, 1425 – 1431.
41. Garside J.; Tavare N. S. Non-isothermal effectiveness factors for crystal growth. *Chem. Eng. Sci.*, **1981**, 36, 863 – 866.
42. Richardson J. F.; Peacock D. G.; *Coulson and Richardson's Chemical Engineering Vol. 3: Chemical & Biochemical Reactors and Process Control* (3rd Ed.), Butterworth-Heinemann, 1994.
43. Borchardt-Setter K. A.; Yao X.; Cersonsky R. K.; Stelzer T.; Chen S.; Sheikh A.; Zhang G. G. Z.; Yu L. Effect of Surfactants on Posaconazole Crystallization and polymorphism: Tween 80 vs Span 80. *Cryst. Growth Des.*, **2025**, 25, 7317 – 7327
44. Czajkowska-Kośnik A.; Sznitowska M. Solubility of ocular therapeutic agents in self-emulsifying oils i. Self-emulsifying oils for ocular drug delivery: solubility of indomethacin, aciclovir and hydrocortisone. *Acta Pol. Pharm.*, **2009**, 66, 709 – 713

For Table of Contents Use Only

Bulk crystallisation of indomethacin from simple and complex solvents

Paul A. Slavin^{a,c}, David B. Sheen^{a,d}, Evelyn E. A Shepherd^a, John N. Sherwood^a, Ranko M. Vrcelj^{a*}

Neil Feeder^{b,d}, Snezana Milojevic^{b,e}

